Study of the optical properties of the amorphous Sb_2S_3 thin films

F. AOUSGI[*], M. KANZARI

Laboratoire de Photovoltaïque et Matériaux Semi-conducteurs-ENIT BP 37, Le belvédère 1002-Tunis, Tunisie

Sb_2S_3 thin films have been deposited by single source vacuum thermal evaporation onto glass substrates at various substrate temperatures in the range 30- 240 °C. The X-ray diffraction spectra indicated that all the as-deposited Sb_2S_3 films were amorphous.The optical constants were obtained from the analysis of the experimental recorded transmission and reflectance spectral data over the wavelength range 300–1800 nm. It has been found that the refractive index dispersion data obeyed the single oscillator of the Wemple–DiDomenico model. By using this model, the dispersion parameters and the high-frequency dielectric constant were determined. The electric free carrier susceptibility and the carrier concentration on the effective mass ratio were estimated according to the model of Spitzer and Fan.

1. Introduction

The study of chalcogenide as Sb_2S_3 thin films has increased in last decades because of their application in the fields of fiber optics, xerography, novel memory devices [1,2] and as photoconductive target for vidicon type of television camera [3, 4]. The interest in the optical properties of amorphous semiconductors has been stimulated also by their possible applications as switching elements and optical transmission media, as well as by their use as passivity materials for integrated circuits [5]. Due to these potential applications it is very important to determine the structural, electrical and optical properties of the material in amorphous phase.

In this paper we report our investigations on the optical properties of amorphous thin films of Sb_2S_3 which were studied in the photon energy range 0-4 eV. The measurements give information regarding the band gap (Eg), refractive index (*n*), absorption index (*k*) and absorption coefficient (*α*), to verify the consistency of the materials for some specific applications. An attempt has been made to highlight the optical features of the alloys in thin film form. So, the dispersion parameters, the high-frequency dielectric constant, the electric free carrier susceptibility and the carrier concentration on the effective mass ratio were estimated according to the model of Spitzer and Fan and Wemple–Di Domenico.

2 Experimental details

2.1 Synthesis of Sb_2S_3 crystal

Stoichiometric amounts of the elements of 99.999% purity antimony Sb and sulphur S were used to prepare the initial ingot of the Sb_2S_3 material. The mixture was sealed in vacuum in a quartz tube. .In order to avoid explosions due to sulfur vapor presses, the quartz tube was heated slowly (20°C/h). A complete homogenization could be obtained by keeping the melt at 650°C for 48 h. The tube was then cooled at the rate 7°C/h. Therefore, cracking, due to thermal expansion of the melt on solidification, was avoided. The compound obtained is dark grayish color. X-ray diffraction of Sb_2S_3 powder analysis showed that only the Sb_2S_3 phase was present in the ingot (Fig. 1) [6]. Crushed powder of this ingot was used as raw material for the vacuum thermal evaporation.
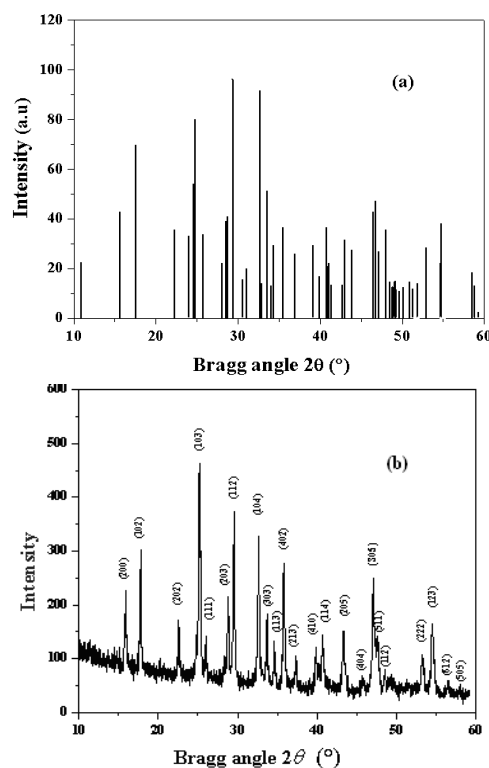

Fig. 1. X-ray diffractogram of the Sb_2S_3 (a): and (b): this work..

2.2 Film preparation

A Tantale crucible (resistivity heated) was used as evaporator source. The pressure of the chamber during evaporation was about 10^{-6} Torr. The substrate temperature was measured using a Chromel–Alumel thermocouple in contact with substrate surface. We noted that the Sb_2S_3 powder was completely evaporated. During this deposit, we have varied the substrate temperature from 30 °C to 240 °C. The obtained films adhere well to the substrates.

This result was in agreement for example with the results of F. Peroles and al [10].

3.2 Optical properties

3.2.1 Optical transmission and reflection spectra

Optical transmission (T) and reflection (R) spectra's of the Sb_2S_3 thin films were recorded at
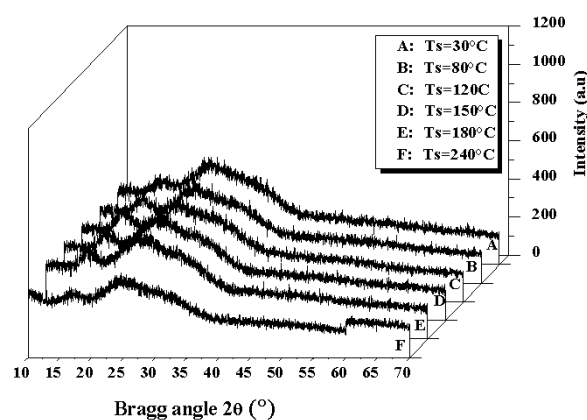

Fig. 2. X-ray diffraction spectra of the Sb_2S_3 thin films deposited on to glass substrates heated at different temperatures in the range 30-240°C.

2.3 Characterization of the as-deposited Sb_2S_3 thin films

The structure of the Sb_2S_3 thin films was determined by means of X-ray diffraction (XRD) using a D8 Advance diffractometer with CuKα radiation (λ=1.5418 Å). Phase identification has been carried out by comparison of the observed d-spacing with the powder diffraction standard card file 78-1347 [7]. The optical characteristics were determined at normal incidence in the wavelength range 300 - 1800 nm using a Shimadzu UV/VIS/NIR-spectrophotometer. The film's thicknesses were calculated from the positions of the interference maxima and minima of reflectance spectra using a standard method [8]. The film thicknesses were found to be in the range 468-648 nm. The type of conductivity of the as-deposited Sb_2S_3 thin

films was determined by the hot probe method and all the as-deposited films present high resistive values.

3. Results and discussion

3.1 Structural properties

Fig. 1 shows the spectra's of the theoretical and the synthesized powders of the Sb_2S_3 material [9]. The powder spectrum confirms that only the Sb_2S_3 phase is present with the preferential orientation following the plane (103).

In the other hand the XRD analysis of the all as-deposited Sb_2S_3 thin films revealed that the all the layers are amorphous as shown in figure 2. different substrate temperatures in the spectral range 400 – 1800 nm. This range covers the fundamental optical absorption edge and the transition regions of the semiconductor materials. The obtained spectra are shown in Fig.3. Swanepoel's formula was used [11] to estimate the optical constants. The transmission and the reflection spectra's show interference patterns with sharp fall of the transmission at the band edge, which is an indication of good homogeneity of the films. The averages of the transmission and the reflection of the all layers in the transparency region (700-1800 nm) are about 70% and 30 % respectively. So no absorption by the free carrier charges is observed in this transparency region since no decrease in the transmission values was occurs.
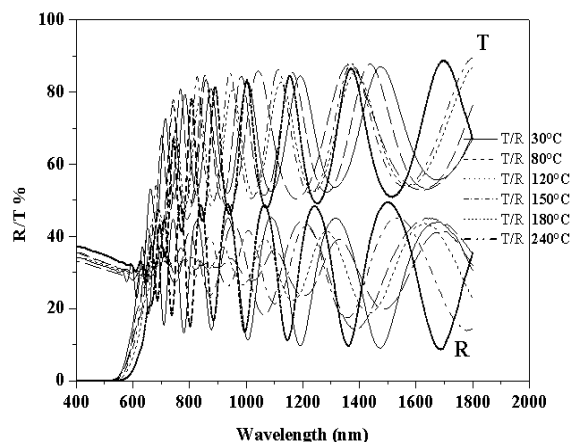

Fig. 3. Optical reflection and transmission spectra of Sb_2S_3 thin films deposited on glass substrates heated for different temperatures between 30-240°C.

3.2.2 Refractive index dispersion analyses

It is known from the dispersion theory that in the region of low and medium absorption the index of refraction n is given in a single oscillator model by the expression [12]

$$n = \left[N + \left(N^2 - S^2 \right)^{\frac{1}{2}} \right]^{\frac{1}{2}}, \qquad (1)$$

where

$$N = 2S \frac{T_M - T_m}{T_M T_m} + \frac{S^2 + 1}{2},$$

S is the refractive index of the quartz substrate and T_M and T_m represent the envelopes of the maximum and minimum positions of the transmission spectra. Exponential variation of T with absorption coefficient α is most probable near the absorption edge. In the present work, the absorption coefficient (α) was calculated using the relation [12, 13]:

$$T = (1 - R)^2 e^{-\alpha d}, \qquad (2)$$

where R is the reflectance, T is the transmittance, α is the absorption coefficient and d is the film thickness. The variation of the absorption coefficient, α, as a function of the photon energy for Sb₂S₃ films for different temperatures are presented in Fig.4. It can be seen that all the films have relatively high absorption coefficients (10^4-10^5 cm^{-1}) in the visible range and near-IR spectral range. This result is very important since the spectral dependence of the absorption coefficient affects the solar conversion efficiency in the case if this material was used as absorber in the solar cells [14].
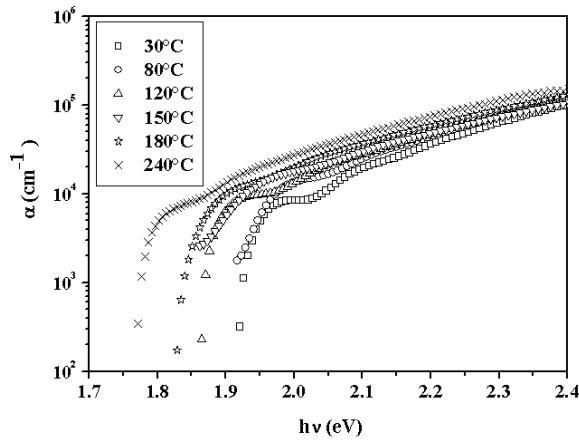

Fig. 4. A plot of the optical absorption coefficient versus the photon energy of the as deposited Sb₂S₃ films.

The relation between the absorption coefficient, α, and the incident photon energy, hυ, can be written as [15, 16]:

$$(\alpha h \upsilon) = A (h \upsilon - E_e)^n, \qquad (3)$$

where A is a constant and n is a number which characterizes the transition process. The value, $n = 1/2$,

characterizes a direct allowed optical transition for the amorphous as-deposited thin films [17]. Plotting of $(\alpha h \upsilon)^2$ versus photon energy, hυ, yields a straight line indicating direct optical transition. All the energy gap values were assembled in the table 1. The direct band gap energy values decrease from 2.08 to 1.86 eV with increasing the substrate temperature. So in our case the substrate temperature has not a great effect on the energy band gap because the films were globally amorphous as we show by X-ray diffraction measurements.

In the spectral region of medium absorption where interference fringes appear distinctly in the transmission spectra, α, is given by [11],

$$\alpha = \frac{1}{d} Ln \left[\frac{(n-1)^3 (n - S^2)}{F - \left[F^2 - (n^2 - 1)^3 (n^2 - S^4) \right]^{\frac{1}{2}}} \right], \quad (4)$$

Where $\quad F = \dfrac{8n^2 S}{T_i}$

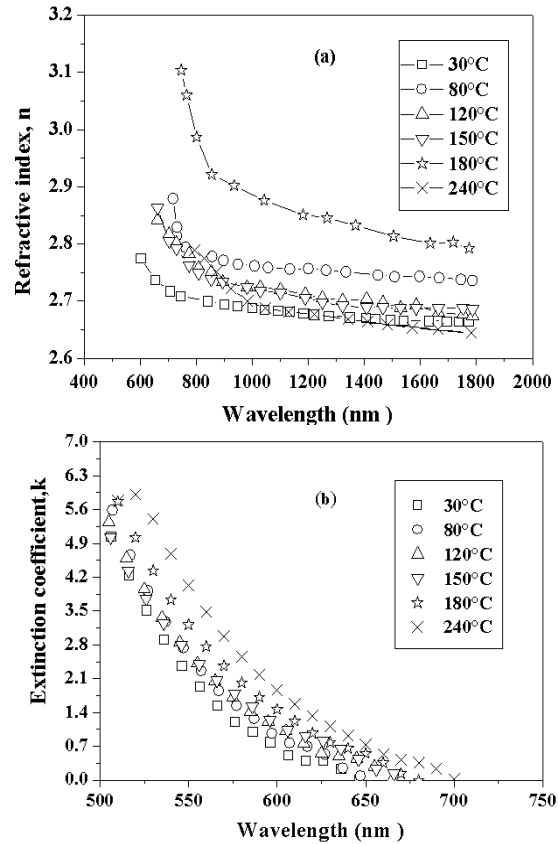And $\quad T_i = 2 \dfrac{T_M T_m}{T_M + T_m}$

Fig. 5. Variation of refractive index n (a) and extinction coefficient k (b) with wavelength for Sb₂S₃ thin films deposited with different substrate temperatures.

Fig. 5a and 5b show the refractive index, n, and the extinction coefficient, k, respectively, for the as-deposited Sb_2S_3 thin film as a function of wavelength. It is clear that the refractive indices variations obey to the Cauchy law [18] for all the films. In addition, the average refractive indices values were in range 2.67 - 2.75 for the all the films except for the films deposited at Ts = 180°C where the average refractive index is 2.85. These refractive indices values were taken for wavelengths greater than 1000 nm which corresponds to the spectral transparency region. It is obviously that the extinction coefficients appear to become important only in the spectral absorption region for wavelengths less than 750 nm.

In the other hand, the data on the dispersion of the refractive index were evaluated according to the single effective oscillator model proposed by Wemple and Di Domenico [19, 20]. It is well known from the dispersion theory that in the region of low absorption the refractive index n described to a very good approximation, by the following formula,

$$n^2(h\nu) = 1 + \frac{E_d E_0}{E_0^2 - (h\nu)^2}, \qquad (5)$$

where, $h\nu$ is the photon energy, E_0 is the single oscillator energy and E_d is the dispersion energy.

Plotting $(n^2-1)^{-1}$ against $(h\nu)^2$ (Fig. 6) allow us to determine the oscillator parameters by fitting a straight line to the points. The values of E_0 and E_d can be determined directly from the slope $(E_0 E_d)^{-1}$ and the intercept on the vertical axis, (E_0 / E_d). It was found that E_d varies between 24.1 and 38.6 eV and E_0 varies from 4 to 6 eV for the different substrate temperatures. The different values of the oscillator parameters were summarized in the table 1. It is well known that the oscillator energy E_0 is to a fair approximation related empirically to the lowest direct band gap Eg: by: $E_0 \approx 2.5 \ E_g$ as found by B. Yous, and al [21]. So in our case the average ratio $E_0/E_g \approx 2.4$ is found which in good accord with the B.Yous and al [21] results.

An empirical relation for dispersion energy in terms of the co-ordination number of cation that is the nearest neighbour to the anion N_c and the effective number of valance electrons per anion N_e can be written as [19]

$$E_d = \beta N_c Z_a N_e, \qquad (6)$$

from this equation the calculated β-factor has the value 0.31 eV, Z_a is the formal chemical valance of the anion. For Sb_2S_3, $Ne = 8$, $Za = 2$ and $N_c = 6$.
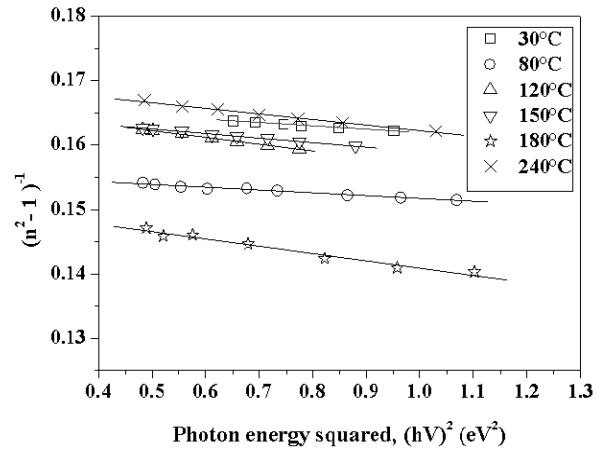

Fig. 6. Plot of $(n^2-1)^{-1}$ versus $(h\nu)^2$ for Sb_2S_3 thin films deposited with different substrate temperatures.

For further analysis of the optical data, the contribution from the free carrier electric susceptibility, χ_e, to the real dielectric constant is discussed according to the Spitzer–Fan model by [21]

$$\varepsilon_r = n^2 - k^2 = \varepsilon_\infty - \left(\frac{e^2}{\pi c^2}\right)\left(\frac{N}{m^*}\right)\lambda^2, \quad (7)$$

and

$$\left(\frac{e^2}{\pi c^2}\right)\left(\frac{N}{m^*}\right)\lambda^2 = -4\pi\chi_e, \qquad (8)$$

where ε_∞ is the high-frequency dielectric constant in the absence of any contribution from free carriers, ε_e is the electric free carrier susceptibility, N/m^* is the carrier concentration to the effective mass ratio, e is the electronic charge, and c is the velocity of light.
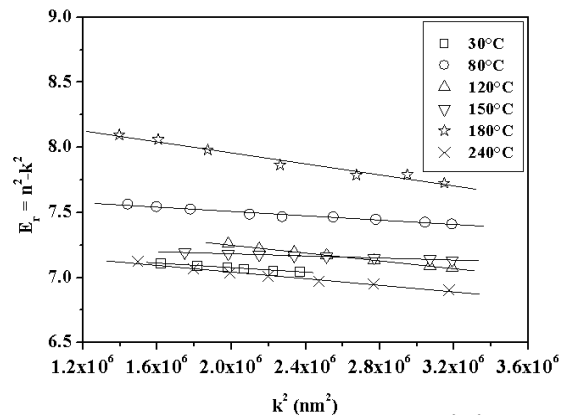

Fig. 7. Plot of optical dielectric constant $\varepsilon_r = n^2 - k^2$ versus wavelength squared λ^2 for Sb_2S_3 thin films deposited with different substrate temperatures.
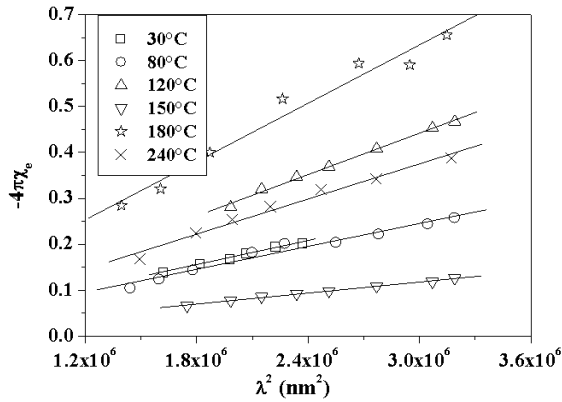
Fig. 8. Plot of (-4πχ$_e$) versus λ for Sb$_3$S$_3$ thin films deposited with different substrate temperatures.

Plotting, ε_r versus λ^2 (Fig. 7), and fitting to a straight line, the values of N/m^* and ε_∞ were estimated. It is important to compare the values of ε_∞ achieved from the Wemple–Di Domenico model (Fig. 6) with that of obtained from Spitzer–Fan model (Fig. 7)., as they show satisfactory agreement. Fig.8 shows (-4πχ$_e$) versus λ^2 in the spectral range 1100–1800 nm. The figure depicts that χ$_e$ increases in magnitude with the wavelength squared and becomes sufficiently large to reduce the refractive index and dielectric constant in the near-infrared region. A good fit to a straight line is seen from which the free carrier susceptibility values at the extremes of the investigated range were estimated. They are listed in Table1.

Table1. The estimated values of the oscillator parameters E$_0$ and E$_d$, the value of the refractive index, n(0), and ε$_\infty$ as well as other related optical parameters extrapolated from the Wemple–Di Domenico model.

T$_s$(°C)	E$_0$ (eV)	E$_d$ (eV)	n(0)	ε$_{\infty sf}$	E$_{\infty wd}$	E_g^{dir} (eV)	E$_0$ / E_g^{dir}	(N /m*) (*10^{48}cm^{-3})	-X$_e$ (*10^{-2})
30	5.71	34.33	2.66	7.25	7,01	2.08	2.74	1.11	1.12~1.61
80	6.02	38.63	2.73	7.67	7,41	2.02	2.98	1.46	0.83~2.05
120	4.07	24.54	2.67	7.54	7,03	1.96	2.07	0.26	2.23~3.71
150	4.86	29.33	2.68	7.26	7,04	1.94	2.5	0.7	0.52~1.01
180	3.66	24.12	2.78	8.38	7,6	1.9	1.92	0.037	2.26~5.22
240	4.45	26.13	2.64	7.29	6,87	1.86	2.39	0.022	1.33~2.02

4. Conclusions

Vacuum thermal evaporation technique was used for the deposition of Sb$_2$S$_3$ thin films on heated glass substrates. The substrate temperatures were varied in the range 30- 240 °C. All the deposited films were amorphous as confirmed by the X-ray diffraction analysis and highly resistive. The refractive index, n, and extinction coefficient, k, of the deposited Sb2S3 films determined from the transmission and reflection spectra's were calculated for all the as-deposited films. The later data allowed the determination of the oscillator strengths, oscillator energies, static refractive indices and static dielectric constants. The refractive index and the single-oscillator parameters were calculated and discussed in terms of the Wemple–DiDmenico model. The values of the high-frequency dielectric constant, the carrier concentration to the effective mass ratio and the electric free carrier susceptibility were also determined using the Spitzer–Fan model. Analysis of the optical absorption data of Sb$_2$S$_3$ films revealed a direct optical transition associated with a band gap energy which decreases from 2.08 to 1.86 eV by increasing the substrate temperature. All the films have relatively high absorption coefficients (10^4- 10^5 cm^{-1}) in the visible range and near-IR spectral range Determination of these parameters may help in technological applications of Sb$_2$S$_3$ in thin film form.

References

[1] R. Zallen, The Physics of Amorphous Solids, Wiley, New York (1983).
[2] A.M. Farid, Egypt. J. Sol. **25**, 1 (2002).
[3] Q. Lu, H. Zeng, Z. Wang, X. Cao, L. Zhang, Nanotechnology, **17**, 2098 (2006).
[4] Z.S. El Mandouh, S. N. Salama, J. Mat. Sci. **25**, 1715 (1990).
[5] S.H. Wemple, Phys. Rev. B. **7**, 3767 (1973).
[6] A. Rabhi, M. Kanzari, B. Rezig, Mater. Lett. **62**, 3576 (2008).
[7] D. O Mckee, J. T. McMullan, Z. Kristallogr, Kristallgeom., Kristallphys., **142**, 447 (1975).
[8] O. S. Heavens, Optical Properties of Thin Solid Films, Butterworths, London (1955).
[9] N. Ghraïri, F. Aousgi, M. Zribi, M. Kanzari, Optoelectron. Adv. Mater. –Rapid Comm., **3**, 8 (2009).
[10] F. Perales, G. Lifante, F. Agullo-Rueda, C. de las Heras, Appl. Phys. **40**, 2440 (2007).
[11] R. Swanepoel, J. Phys. E, **16**, 1214 (1983).
[12] J. I. Pankove, Optical processes in semiconductors, Prentice-Hall, New Jersey (1971).
[13] D. E. Milovzorov, A. M. Ali, T. Inkuma, Y. Kurata, T. Suzuki, S. Hasegawa, Thin Solid Films **382**, 47 (2001).

[14] V. V. Kindyak, V. F. Gremenok, I. V. Bodnar, V. Yu Rud, G. A. Madvedkin, Thin Solid Films **250**, 33 (1994).

[15] N. F. Mott, E. A Davis, Electronic Progresses in Non-Crystalline Material, Oxford University Press, New York (1971).

[16] J. T. Tauc, Amorphous and Liquid Semiconductors Plenum Press, New York (1974).

[17] E. A. El-Sayad, G. B.Sakr, Cryst. Res. Technol. **40**, 1139 (2006).

[18] K. Prabakar, S. Venkatachalam, Y. L. Jeyachandran, Sa. K. Narayandass, D. Mangalaraj, Sol. Energy Mater. Sol. Cells **81**, 1 (2004).

[19] S. H. Wemple, M. DiDomenico; J. Phys. Rev. B **3**, 1338 (1971).

[20] S. H. Wemple, Phys. Rev. B. **7**, 3767 (1973).

[21] B. Yous, J. M. Berger, J. P. Ferraton Eta. Donnadien, Thin Solid Films, 82, 279 (1981).

[22] W. G. Spitzer, H. Y. Fan, Phys. Rev. **106**, 882 (1957).

---

[*]Corresponding author: aousgifethi@yahoo.fr